BULLETIN OF THE POLISH ACADEMY OF SCIENCES
TECHNICAL SCIENCES, Vol. 71(3), 2023, Article number: e144615
DOI: 10.24425/bpasts.2023.144615

Human-induced force reconstruction using a non-linear electrodynamic shaker applying an iterative neural network algorithm

César PELÁEZ-RODRÍGUEZ[1,2]*, **Álvaro MAGDALENO**[2], **Sancho SALCEDO-SANZ**[1], **and Antolín LORENZANA**[2]

[1] Department of Signal Processing and Communications, Universidad de Alcalá, Alcalá de Henares, 28805, Spain
[2] ITAP. Escuela de Ingenierías Industriales. Universidad de Valladolid. P.º del Cauce, 59, 47011 Valladolid, Spain

Abstract. An iterative neural network framework is proposed in this paper for the human-induced Ground Reaction Forces (GRF) replication with an inertial electrodynamic mass actuator (APS 400). This is the first approach to the systematization of dynamic load tests on structures on a purely objective, repeatable and pedestrian-independent basis. Therefore, an inversion-free offline algorithm based on Machine Learning techniques has been applied for the first time on an electrodynamic shaker, without requiring its inverse model to tackle the inverse problem of successful force reconstruction. The proposed approach aims to obtain the optimal drive signal to minimize the error between the experimental shaker output and the reference force signal, measured with a pair of instrumented insoles (Loadsol©) for human bouncing at different frequencies and amplitudes. The optimal performance, stability and convergence of the system are verified through experimental tests, achieving excellent results in both time and frequency domain.

Key words: ground reaction forces; electrodynamic shaker; artificial neural networks; forces reconstruction; iterative neural network.

1. INTRODUCTION

The effects of human induced forces over structures are increasingly gaining importance as modern structures become lighter, slenderer and with lower natural frequencies that are excited by regular human activities, such as walking or running [1, 2]. Therefore, it becomes necessary to periodically assess the structures with serviceability tests. Nonetheless, the tendency of pedestrians to modify their walking pattern when walking on a vibrating surface, with the aim of maximizing their comfort, causes a great lack of repeatability in the transits, even when conducted in a controlled environment, or when a timing device is used to perform repeated experiments [3]. This issue considerably hampers the execution of these tests, preventing a direct comparison between structures or the evaluation of the installation of vibration mitigation devices.

This paper arises as a response to this issue, establishing a preliminary approach to the systematization of dynamic load tests on structures on a purely objective, repeatable and pedestrian-independent basis. To this end, an electrodynamic shaker [4] has been used to recreate the Ground Reaction Forces (GRFs) produced by humans, whose temporal signals were previously acquired with a pair of instrumented insoles. This shaker consists of an inertial actuator, which works by generating inertial forces on the structure on which it is placed. The replication of the dynamic component of the GRF is precisely the interest of this work. The inertial shaker employed represents an inherently nonlinear electro-mechanical system [5] whose dynamics are modeled with a non-invertible model [6]. This causes the inverse problem of obtaining the shaker drive target signal (the one which makes the actuator behaves as desired) to be not straightforward.

Solutions to similar problems may be found in the literature. First of all, adaptive control techniques have been extensively applied in earthquake simulations by means of shaking tables [7–10]. These adaptive techniques have also been explored in the field of humanoid robots [11–14]. Another classical alternative consists of using an iterative learning control system (ILC) [15, 16]. The application of this control method to shaking tables has been explored in [17–19]. Regarding the model inversion, the possibilities present in the literature include classical inversion [20, 21], stable inversion [22], adjoint systems [23], robust ILC designs [24] or some modeling-free inversion-based approaches [25]. Recently, a new trend has emerged, in which data-driven techniques are employed as an alternative to the classical control methods. This represents the possibility of avoiding a complex model inversion by means of Machine Learning (ML) algorithms [26–28, 28, 29].

The approach adopted in this paper consists of the development of an iterative ML data-driven framework. Specifically, an Artificial Neural Network (ANN) is used as a regressor to generate off-line the optimal drive signal that makes the shaker follow a specific reference force signal. As the shaker is an inertial mechanical system, in order to output the voltage signal

*e-mail: cesar.pelaez@uah.es

Manuscript submitted 2022-09-30, revised 2022-11-22, initially accepted for publication 2022-12-20, published in June 2023.

at each temporal instant, the ANN is fed with data relative to both the future reference force and the conditions of the moving mass at previous instants. Iteratively, the simulated force signal is compared to the reference, and the most optimal points (those whose error is below a previously defined threshold) are selected as training data for the following iteration. This way, the ANN weights are updated at each iteration, allowing the drive signal to converge to an optimal value, as demonstrated via experimentation. Since the network is only trained with data within the optimal operating range of the shaker, its output will be constrained within this range, ensuring the stable operation of the system.

The main contributions of the manuscript are described as follows: first, an inversion-free, offline control methodology based on ML has been applied to an electrodynamic shaker for the first time, achieving very convincing results in both time and frequency domain. Second, the work presented in this paper supposes a first step in the systematization of dynamic load tests on structures on a purely objective, repeatable and pedestrian-independent basis.

The rest of the manuscript has been organised as follows: In Section 2, the material resources employed in the experimental work of this paper are detailed. In Section 3, the proposed methodology is exhaustively described. The experimental validation of this framework is reported in Section 4. Finally, the discussion and conclusions, together with suggestions for future work, are set out in Section 5.

2. MATERIALS AND METHODS

The material resources employed in the realization of this paper are detailed below. These are the instrumented insoles used for the acquisition of the reference GRFs (Section 2.1) and the electrodynamic shaker used to replicate the temporal force signals (Section 2.2).

2.1. Wireless instrumented insoles

The experimental GRF data acquisition for subsequent replication was performed using a pair of wireless instrumented insoles recently developed by Novel Gmbh (Munich, Germany) [30, 31]. This Loadsol© insole sensor (Fig. 1) was designed to estimate the GRF by directly measuring the total normal force at the plantar surface of the foot and the shoe. Loadsol© uses a highly ergonomic and linearly sensitive capacitor-based sensor that spans the entire plantar surface of the foot. This means that force is detected perpendicular to the foot, irrespective of the location at which it is applied. The sensor is attached by a thin flexible band to a small electronics unit clipped to the top or lateral side of the shoe. Force data are recorded at 100 Hz and transmitted in real-time wirelessly to a smart device via a Bluetooth connection for storage, review and app-based analysis. The accuracy and precision of this force measurement device have been assessed in [32, 33].

Fig. 1. Wireless instrumented insoles

2.2. Electrodynamic shaker

The inertial mass electrodynamic shaker APS 400 ELECTRO-SEIS [4] (Fig. 2) was employed for GRF replication. The main application of these devices consists of the induction of inertial forces in structures when undertaking dynamic tests. The actuator consists of a mobile reaction mass attached to a current coil that moves in a magnetic field created by an array of permanent magnets. The moving mass is connected to the frame by a suspension system, modeled by a spring stiffness and a viscous damping. It is fed by an electrical signal that varies in voltage between ± 5 V; this signal is usually either a noise signal or a sinusoidal one.

Fig. 2. Inertial electrodynamic mass actuator

The dynamics of this type of inertial mass actuators can be described according to the third order transfer function (between generated forces and voltage input) given in equation (1), where K_A corresponds to the transducer constant (in N/A), ω_A is the natural frequency associated with the suspended moving mass system, ξ_A represents the damping coefficient and the pole at ε accounts for the low-pass filtering property of these instruments, absorbing frequencies higher than the cut-off frequency ε (in rad/s) [6].

$$G_A(s) = \left(\frac{K_A s^2}{s^2 + 2\xi_A \omega_A s + \omega_A^2}\right) \cdot \left(\frac{1}{s+\varepsilon}\right). \tag{1}$$

The process of obtaining the model parameters consists of applying a curve-fitting algorithm (Matlab lsqnonlin function) so that the experimental and analytical Frequency Response Function (FRF) presents the minimum possible error. The experimental FRF was calculated by applying a 60000-point Blackman window over the experimental data obtained by applying white noise as the input voltage signal to the shaker in the range of ± 5 V, with a test duration of 10 minutes and a sampling frequency of 1000 Hz. The experimental acceleration was measured with piezoelectric accelerometers (IEPE) from MMF (Metra Mess und Frequenztechnik). The manual gain position of the amplifier corresponds to 25% of the maximum gain. The values determined for each parameter are ($K_A = 4113$ N/V, $\omega_A = 15.02$ rad/s (2.39 Hz), $\xi_A = 0.23$ and $\varepsilon = 62.08$ rad/s

(9.89 Hz). Figure 3 shows the comparison between the experimental and the modeled FRF. Note the small fluctuation in the experimental FRF magnitude at frequencies near 0 Hz due to the measurement range of the accelerometers used, which starts at 0.16 Hz.

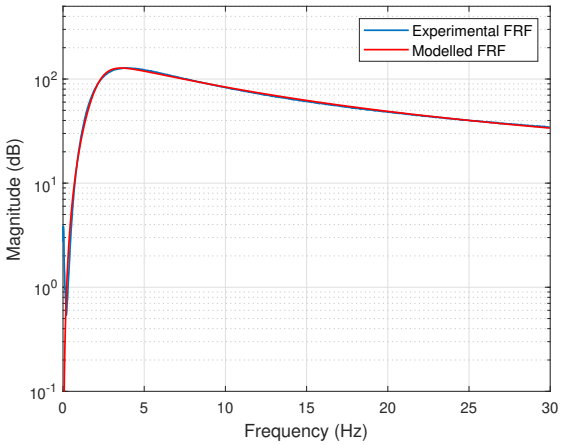

Fig. 3. Transfer function of the actuator $G_A(s)$: magnitude in dB referenced to 1 N/V

3. PROPOSED FRAMEWORK

This section provides a detailed description of the proposed methodology, based on an iterative ANN framework, for the replication of a reference GRF. Figure 4 illustrates the workflow of this methodology, where a reference time force signal is entered as input, and a voltage drive signal is returned as output. Subsequently, this optimum drive signal is fed to the inertial shaker to obtain the corresponding experimental GRF.

In this workflow, an external loop and an internal loop can be differentiated. First, the ANN training is performed with a backpropagation algorithm in the outer loop. Initially, the network is trained with random values and ramps between the maximum and minimum voltage (± 4 V), generating a voltage data buffer that will be updated at each iteration in order to train the network with increasingly specific data (with a maximum buffer size of $L = 50000$ samples to avoid excessive training time when accumulating several iterations). The structure of the ANN input is defined as follows: the first m entries $(X_{1:m})$ provide the ANN with information about the future actions that will be demanded and the remaining inputs provide the ANN with information about the shaker status in the previous instants, both in voltage $(X_{m+1:2m})$ and force generated $(X_{2m+1:3m})$, where m is a tunable parameter of the algorithm. The processing treatment of the voltage time signal for acquiring the $(X_{\text{train}}, Y_{\text{train}})$ pairs is depicted in Fig. 6 and involves: (1) the simulation of the shaker direct model to obtain the simulated force signal; (2) the generation (from $i = m+1$ to $i = L-m$) of a matrix of output data (V_i) associated to the corresponding matrix of input data $(F_{i:i+m}, V_{i-m:i-1}, F_{i-m:i-1})$.

Then, the process consists of iteratively feeding an ANN with data relative to both the reference signal at future points and the previous instants of the inertial shaker (voltage and simulated

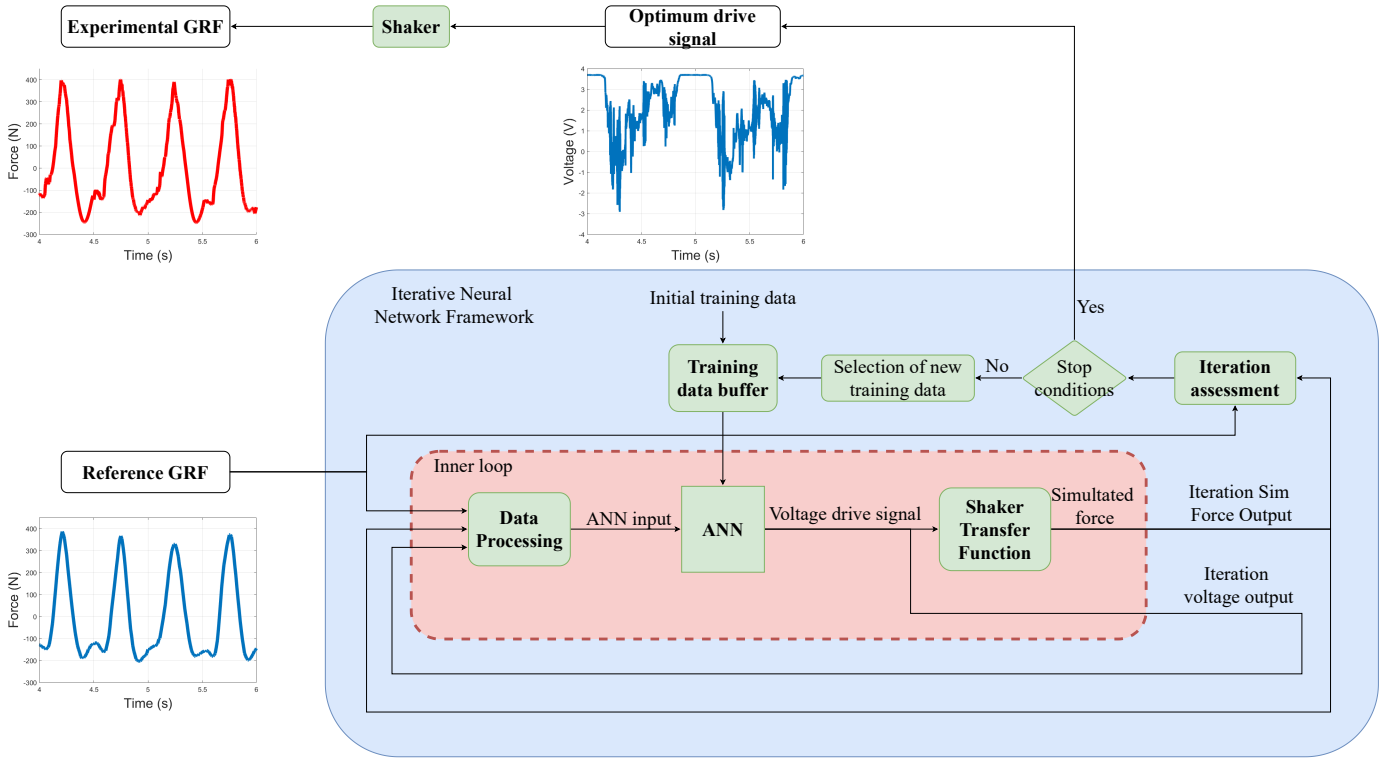

Fig. 4. Iterative Neural Network framework proposed for GRF replication

force). This is accomplished inside the inner loop from $i = 0$ to $i = N$, N being the number of points of the reference GRF signal. The selected architecture for the ANN is a MultiLayer Perceptron (MLP) [34] with a hidden layer. This ANN operates as a regressor where, at each call of the inner loop, the voltage value of that specific point (V_i) is retrieved. The inputs of this network are defined as: the reference force between instants i and $i+m$ and the previous voltage, and the simulated force between instants $i-m$ and $i-1$, where m has been set at 500 after several tests. Figure 5 displays the architecture of the ANN implemented (with $m = 5$ for legibility purposes), indicating which information corresponds to each ANN input. In this loop, the simulated force is calculated by simulation of the shaker direct model (equation (1)) after applying the voltage between 1 and i for that iteration.

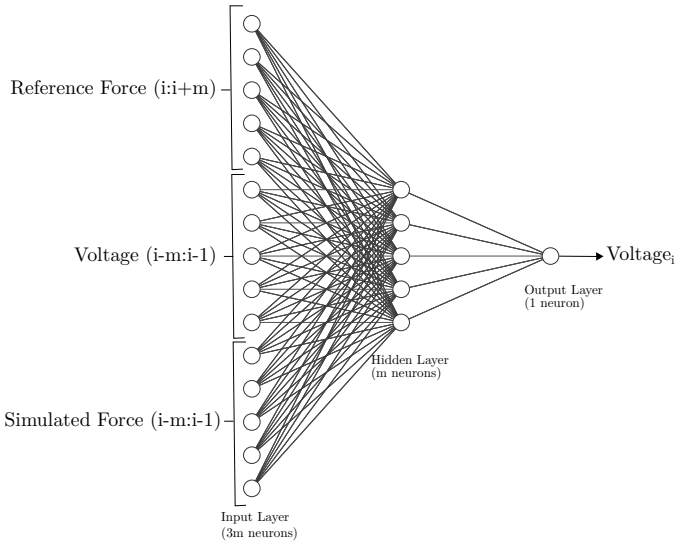

Fig. 5. Implemented ANN structure

Once the entire drive signal (from 1 to N) has been obtained, the corresponding simulated force signal is compared with the reference GRF, the framework variables are updated (minimum error, optimum drive signal and number of iterations without improvement), and the stop condition is evaluated, this being the comparison of the maximum number of iterations without improvement regarding the established limit (5 iterations). The Root Mean Square Error (RMSE) (Equation (2)) between the two force signals is considered as the performance criterion.

$$RMSE = \sqrt{\frac{\sum_{i=1}^{N} (F_{\text{ref}_i} - F_{\text{sim}_i})^2}{N}}. \tag{2}$$

If the stop conditions are not met, we then proceed to the refinement of the ANN training data by selecting the optimal points of that iteration (those in which the error committed is below a threshold set at ± 10 N).These points are added to the training data buffer, and the network is trained again with the new data prior to entering the next iteration. The role of this buffer is to limit the number of training data so that the training time does not drastically rise as the number of iterations increases. In this way, a maximum buffer size ($L = X$) is set and, once it is filled, the new data entering the buffer at each iteration replaces the oldest data.

Finally, when stop conditions are met, the optimum drive signal is provided by the algorithm. This signal is then fed to the shaker in order to obtain the experimental replication of the reference GRF.

4. EXPERIMENTAL WORK

The experimental work carried out in the development of this paper is described in this section. First, the process of acquiring the experimental GRFs is described (Section 4.1), then the simulation results provided by the developed algorithm are shown (Section 4.2), and finally, the experimental GRFs replicated with the shaker are displayed (Section 4.3). Figure 7 shows the experimental framework carried out in the paper.

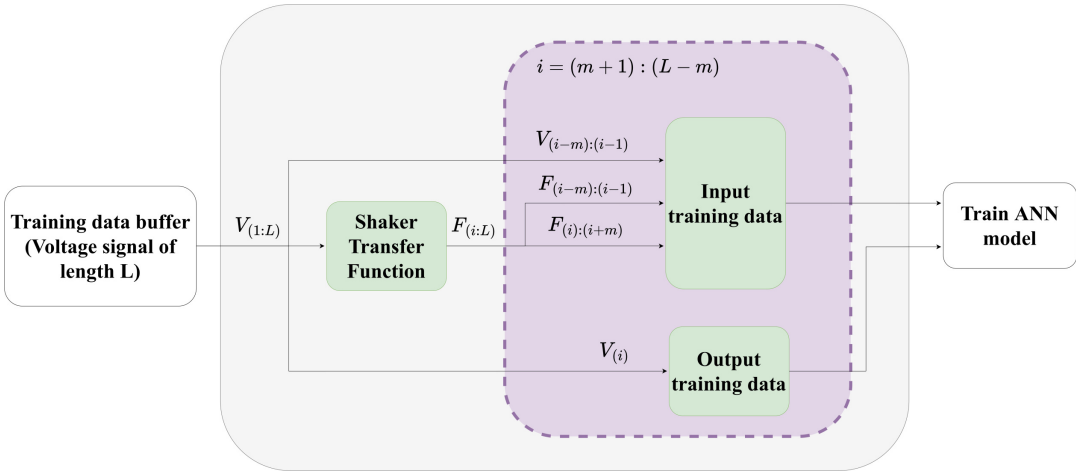

Fig. 6. ANN training procedure

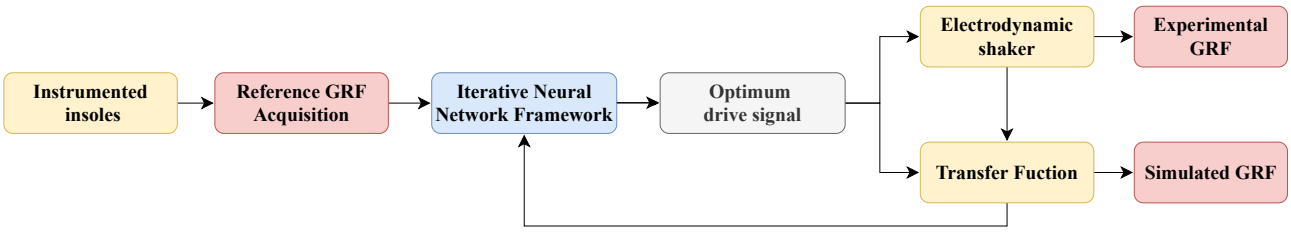

Fig. 7. Experimental framework diagram

4.1. GRF data acquisition

The black lines in Fig. 8 show the 8 different experimental GRFs acquired with the Loadsol© insoles. In order to facilitate the replication of these signals with the shaker, and bearing in mind that the shaker can only apply forces in a single location, only bouncing movements were captured at different frequencies (ranging from 1 to 2.5 Hz) and different amplitudes (meaning the force that the subject exerted while bouncing). All measurements were taken for a duration of 15 seconds by a male, 192 cm tall and weighing 77 kg.

The recorded signals were imported into MATLAB© and preprocessed by summing the signals from both feet and resampling the resulting force signal to 1000 Hz. Also, since the interest of the work resides in the dynamics of the structure on which the force is applied, the static part of the GRFs is removed by subtracting an offset and centering the signals at 0 N. This allows the shaker to accurately reproduce the dynamic loads of the signals.

4.2. Simulation work

The proposed framework was implemented through a MATLAB© R2020a script, where user interface consists of defining the required algorithm parameters (ANN hyperparameters, number of points for each input (m), training voltage buffer length (L), error tolerance, number of maximum iterations and maximum voltage) and inputting both the shaker dynamics model and the file (.txt) with the reference force to be replicated directly extracted from the Loadsol© app. The parameters used for the execution are shown in Table 1, including both the ANN hyperparameters and the algorithm parameters. The maximum voltage value is determined by computing the shaker moving mass displacement, integrating twice the simulated acceleration signal obtained by simulating the model with the drive signal as input. Hence, a maximum voltage is chosen that makes the moving mass move within the limited displacement range of the shaker (±8 cm), avoiding the collision of the moving mass with the end of the stroke limits. Figure 9 shows the expected displacement for each of the experiments compared to the experimental displacements (computed by integrating the measured acceleration twice).

Table 2 shows the results of the algorithm execution, where the RMSE, the OPR (Optimal Points Ratio) (meaning the percentage of points of the simulated signal within the error tolerance of ±10 N), and the iteration number in which the most optimal solution was obtained are shown for each experiment.

Table 1
Implemented algorithm parameters

ANN hyperparameters	Value
Number of layers	1
Neurons per layer	500
Training function	Resilient Backpropagation
Maximum training epochs	10000
Training maximum fails	500
Training ratio	85%
Test ratio	15%
Activation function	Log-sigmoid
Perform function	MSE
Algorithm parameters	**Value**
Number of points for each input (m)	500
Training data buffer length (k)	50000
Error tolerance [N]	10
Number of maximum iterations	7
Assessment criteria	RMSE
Maximum voltage [V]	3.7

Table 2
Simulation results

Exp	RMSE	OPR	Iter.	RMSE slope	OPR slope
Exp 1	51.06	21.98	1.90	–41.11	–6.48
Exp 2	82.07	14.78	4.20	–40.96	1.52
Exp 3	19.36	58.72	13.60	–35.56	3.62
Exp 4	118.20	5.21	3.80	–92.55	–0.39
Exp 5	34.14	24.24	1.50	–13.45	3.42
Exp 6	38.33	35.40	21.00	–25.52	1.54
Exp 7	38.80	21.27	5.50	–29.05	2.49
Exp 8	44.14	26.34	9.40	–32.44	2.53
Mean	53.26	25.99	7.61	–38.83	1.03

In order to ensure the repeatability of the results, and considering the heuristic nature of the training algorithm selected for the ANN, the algorithm was executed 5 times for each experiment, showing the average values in the table. An average value of 62.72 N of RMSE, 25.99% of optimal points, and 7.61 iterations are achieved. In addition, aiming to assess the convergence ratio of the iterative framework, the table shows the

evolution of the RMSE and the OPR throughout the iterations, observing an average improvement of -38.83 N and 1.03% per iteration, respectively. (Note that the negative evolution in the OPR metric is explained by the fact that the assessment criteria in the iterative algorithm is defined as the RMSE, so it is possible that an iteration could present a better RMSE than the previous one, but a worse OPR).

Figure 8 depicts the simulated GRFs compared to the references, showing the accurate prediction yielded in all the experiments. It is possible to notice how experiments 2 and 4, which present RMSE values very superior to the rest of the experiments, show the least satisfactory results when comparing the time signals, particularly for Exp 4. This is due to the fact that the reference force signals exceed the working limits of ±400 N of the electrodynamic shaker in both experiments. Therefore, the algorithm tries to reach the maximum possible force without the shaker moving mass impacting the end-of-stroke limits.

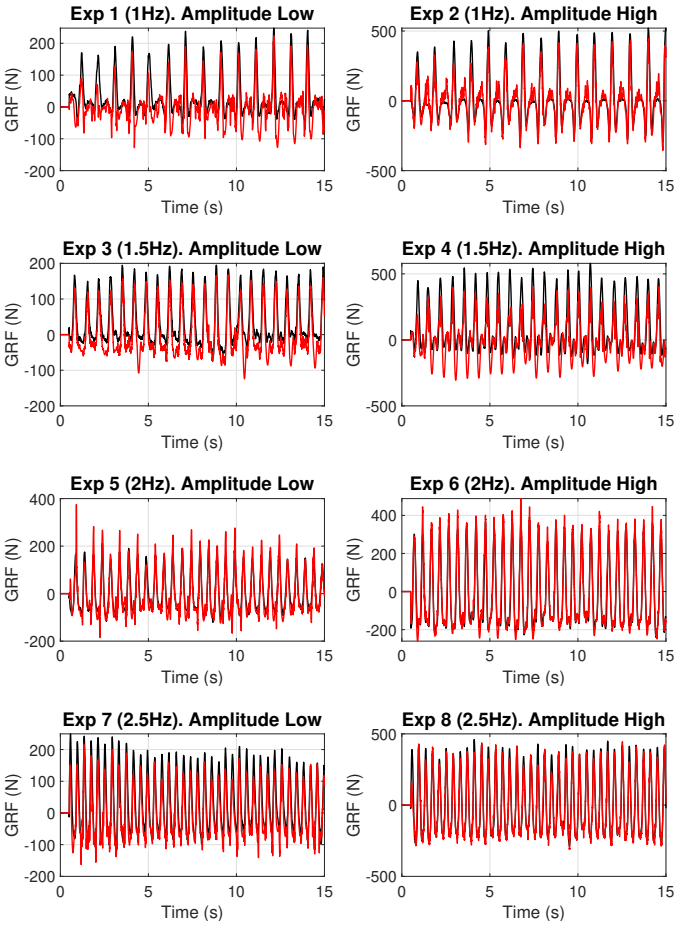

Fig. 8. Simulated GRFs (red) compared to the reference force signals (black)

4.3. Experimental results

Once the drive signals have been optimized for each of the experiments, they are fed to the inertial shaker and the experimental output force is calculated by measuring the acceleration of the shaker moving mass with a piezoelectric accelerometer and multiplying it by the value of this moving mass (31.2 kg). Since the shaker direct model is highly reliable (Fig. 3), the error between the experimental and simulated GRFs is minimal, exhibiting an average correlation coefficient of 0.96 (Table 3). Figure 9 displays a comparison between the expected displacement of the shaker moving mass and the experimental displacement, both computed by integrating twice the simulated and experimental acceleration signals. This demonstrates that both time signals are very similar and that, during the GRF replication, the shaker never reaches its end-of-stroke limits.

Table 3
Correlation coefficients between experimental and simulated GRFs

Exp	c	Exp	c
Exp 1	0.95	Exp 5	0.97
Exp 2	0.98	Exp 6	0.98
Exp 3	0.95	Exp 7	0.95
Exp 4	0.94	Exp 8	0.99
		Mean	0.96

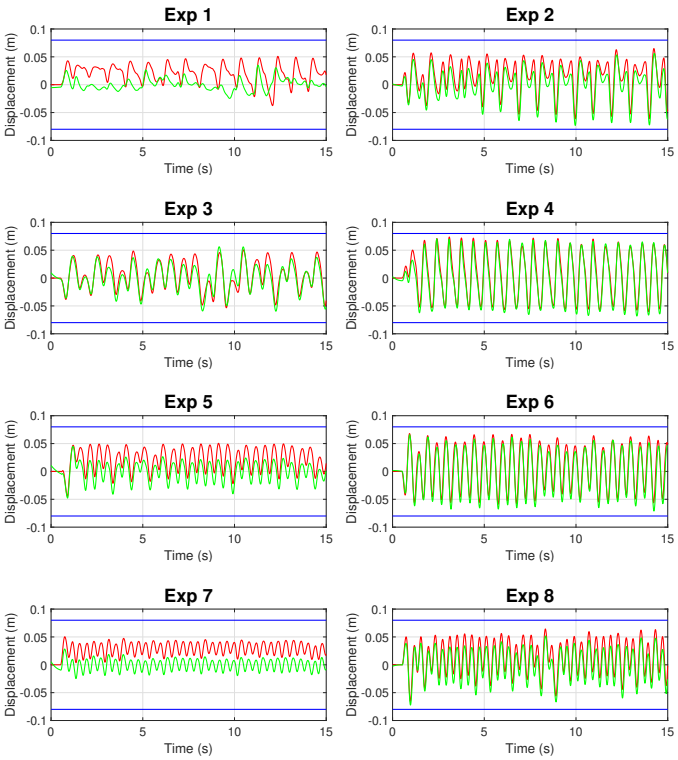

Fig. 9. Integrated displacement of the shaker moving mass (green) compared to the expected displacement computed by simulation (red)

Furthermore, Fig. 10 shows the experimental GRFs performed with the electrodynamic shaker compared to both the simulated and reference GRFs. It can be seen how the replication is extremely accurate for all the experiments, except for Exp 1, which can be explained by observing the FRF of the shaker in Fig. 3: there, it is found that the amplitude of the system at low frequencies is much lower than near the natural frequency

(2.39 Hz), which reduces the ability to replicate forces at very low frequencies. In addition, this effect is intensified when performing the bouncing with low amplitudes, resulting in a reference signal that is far away from a sinusoidal signal, causing the shaker to struggle when replicating high forces values starting from values close to zero, since it does not get enough inertia.

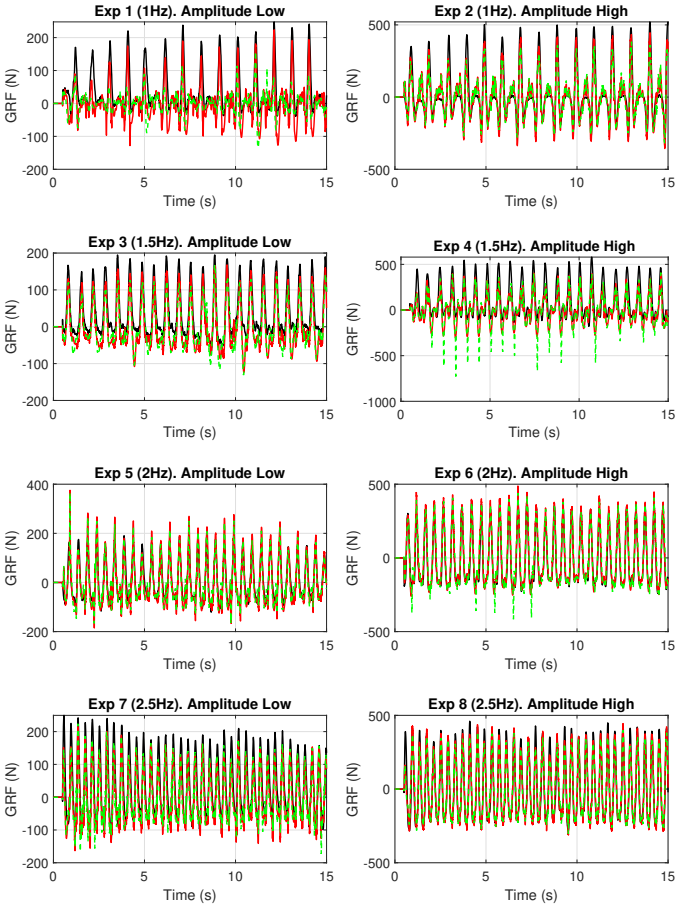

Fig. 10. Experimental GRFs performed with the inertial shaker (green) compared with the simulated GRFs (red) and with the reference force signals (black)

The experimental GRFs are also compared to the reference signals (the ones measured with the insoles) in the frequency domain in Fig. 11. Here, it can be appreciated how the frequency content of both signals is similar, despite certain differences in the amplitudes. Small errors in the time domain signal replication are translated into the frequency domain by slight differences in amplitudes. This means that when the GRFs are reproduced with the shaker on a structure, the same frequencies are excited as if the forces were applied by the human subject.

5. CONCLUSIONS

An ML-based framework for Ground Reaction Forces (GRFs) replication using an electrodynamic shaker has been proposed and successfully implemented in this paper. Its performance was assessed through the replication of 8 temporal signals ac-

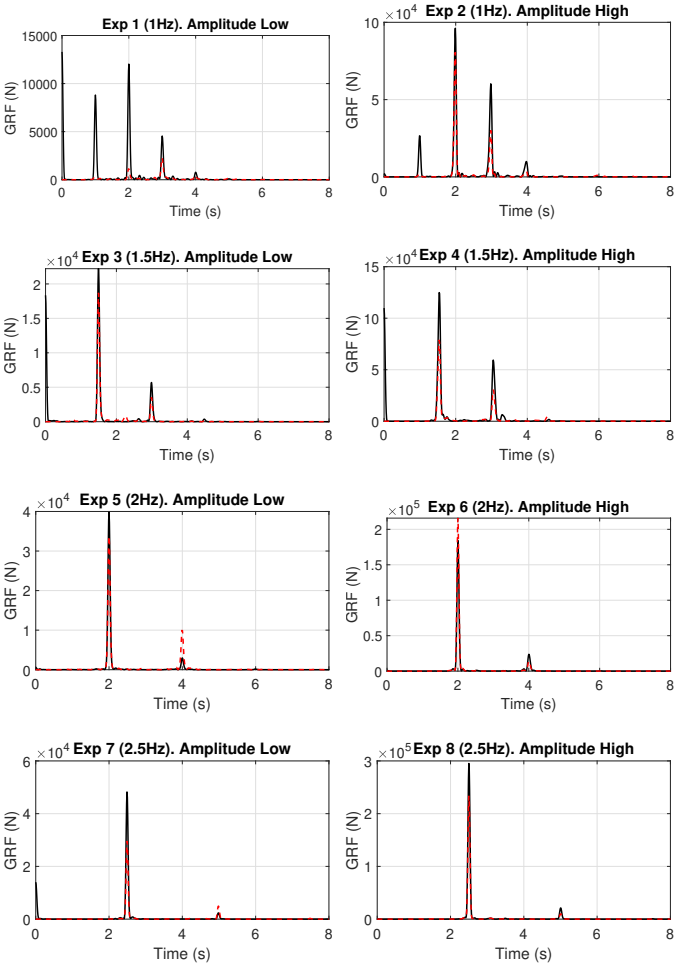

Fig. 11. Frequency domain comparison: Reference human signals (black) and reproduced with the shaker (red)

quired via a pair of instrumented insoles during bouncing at different frequencies and amplitudes. The methodology accurate performance has been accounted both in the time and frequency domain, achieving remarkable results of 53.26 N of average RMSE, an average percentage of 25.99% points of the experimental signal within the error threshold of ± 10 N, and proving a very similar frequency content between the reference GRF acquired with the insoles and the experimental GRF performed with the shaker. This means that when introducing these forces as excitation in a structure, a similar response will be produced, which is the final objective of this paper.

The approach adopted in this paper contributes to provide an efficient alternative to classical control techniques for inverse problems. It provides an inversion-free solution and ensures the stability of the system, as long as the direct actuator model is stable, since the drive signal output from the neural network will always be within the voltage limits at which the shaker operates properly.

Furthermore, the proposed framework is a preliminary approach to the systematization of dynamic load tests on structures on a purely objective, repeatable and pedestrian-independent basis, leading to the possibility of performing serviceabil-

ity tests without requiring skilled people. Future lines of work include: (1) the study of human-structure interaction phenomena from a more experimental approach, making it possible to observe and learn from the differences between the structure response when excited by the shaker and by a pedestrian; (2) endowing the electrodynamic shaker with movement along the structure will allow us to reproduce not only stationary human activities, but also other movements involving locomotion.

ACKNOWLEDGEMENTS

This research has been partially funded by the Spanish Government and the European Union, through the research project number RTI2018-098425. This research has also been partially supported by the project PID2020-115454GB-C21 of the Spanish Ministry of Science and Innovation.

REFERENCES

[1] S. Živanović, I. Diaz, and A. Pavić, "Influence of walking and standing crowds on structural dynamic properties," in *Proceeding of conference & exposition on structural dynamics (IMAC XXVII)*, 2009.

[2] G. Busca, A. Cappellini, S. Manzoni, M. Tarabini, and M. Vanali, "Quantification of changes in modal parameters due to the presence of passive people on a slender structure," *J. Sound Vibr.*, vol. 333, no. 21, pp. 5641–5652, 2014.

[3] C.Y. Tuan and W.E. Saul, "Loads due to spectator movements," *J. Struct. Eng.*, vol. 111, no. 2, pp. 418–434, 1985.

[4] M.A. Peres, R.W. Bono, and D.L. Brown, "Practical aspects of shaker measurements for modal testing," in *Proceedings of ISMA*, 2010, pp. 2539–2550.

[5] A. Saraswat and N. Tiwari, "Modeling and study of nonlinear effects in electrodynamic shakers," *Mech. Syst. Signal Proc.*, vol. 85, pp. 162–176, 2017.

[6] C.M. Casado, I.M. Díaz, J. de Sebastián, A.V. Poncela, and A. Lorenzana, "Implementation of passive and active vibration control on an in-service footbridge," *Struct. Control. Health Monit.*, vol. 20, no. 1, pp. 70–87, 2013.

[7] W. Guo, P. Shao, H.-y. Li, Y. Long, and J.-f. Mao, "Accuracy assessment of shake table device on strong earthquake output," *Adv. Civ. Eng.*, vol. 2019, p. 9372505, 2019.

[8] G. Shen, G.-M. Lv, Z.-M. Ye, D.-C. Cong, and J.-W. Han, "Implementation of electrohydraulic shaking table controllers with a combined adaptive inverse control and minimal control synthesis algorithm," *IET Contr. Theory Appl.*, vol. 5, no. 13, pp. 1471–1483, 2011.

[9] T. Yachun, P. Peng, Z. Dongbin, and Z. Yi, "A two-loop control method for shaking table tests combining model reference adaptive control and three-variable control," *Front. Built Environ.*, vol. 4, p. 54, 2018.

[10] D.P. Stoten and E.G. Gómez, "Adaptive control of shaking tables using the minimal control synthesis algorithm," *Philos. Trans. R. Soc. Lond. Ser. A-Math. Phys. Eng. Sci.*, vol. 359, no. 1786, pp. 1697–1723, 2001.

[11] X. Yu, B. Li, W. He, Y. Feng, L. Cheng, and C. Silvestre, "Adaptive-constrained impedance control for human-robot co-transportation," *IEEE Trans. Cybern.*, vol. 52, no. 12, pp. 13 237–13 249, 2022.

[12] J.T. Vughuma and O. Verlinden, "Control algorithm for an active ankle-foot orthosis (aafos) adaptative admittance control," in *Proceedings of the 2019 6th International Conference on Biomedical and Bioinformatics Engineering*, 2019, pp. 91–98.

[13] L. Almeida, V. Santos, and J.P. Ferreira, "Improved humanoid gait using learning-based analysis of a new wearable 3d force system: Work programme," in *2019 14th Iberian Conference on Information Systems and Technologies (CISTI)*. IEEE, 2019, pp. 1–4.

[14] X. Yu, W. He, Q. Li, Y. Li, and B. Li, "Human-robot co-carrying using visual and force sensing," *IEEE Trans. Ind. Electron.*, vol. 68, no. 9, pp. 8657–8666, 2020.

[15] H.-S. Ahn, Y. Chen, and K.L. Moore, "Iterative learning control: Brief survey and categorization," *IEEE Trans. Syst. Man Cybern. Part C-Appl. Rev.*, vol. 37, no. 6, pp. 1099–1121, 2007.

[16] D.A. Bristow, M. Tharayil, and A.G. Alleyne, "A survey of iterative learning control," *IEEE Control Syst. Mag.*, vol. 26, no. 3, pp. 96–114, 2006.

[17] Y. Tang, G. Shen, Z.-C. Zhu, X. Li, and C.-F. Yang, "Time waveform replication for electro-hydraulic shaking table incorporating off-line iterative learning control and modified internal model control," *Proc. Inst. Mech. Eng. Part I-J Syst Control Eng.*, vol. 228, no. 9, pp. 722–733, 2014.

[18] K. Seki and M. Iwasaki, "Modeling and disturbance compensation aided by multibody dynamics analysis in shaking table systems," *Mech. Eng. J.*, vol. 2, no. 5, pp. 15–00 274, 2015.

[19] Y. Tian, T. Wang, Y. Shi, Q. Han, and P. Pan, "Offline iterative control method using frequency-splitting to drive double-layer shaking tables," *Mech. Syst. Signal Process.*, vol. 152, p. 107443, 2021.

[20] B. Widrow, "Adaptive inverse control," in *Adaptive Systems in Control and Signal Processing 1986*. Elsevier, 1987, pp. 1–5.

[21] L. Silverman, "Inversion of multivariable linear systems," *IEEE Trans. Autom. Control*, vol. 14, 3, pp. 270–276, 1969.

[22] S. Devasia, D. Chen, and B. Paden., "Nonlinear inversion-based output tracking," *IEEE Trans. Autom. Control*, vol. 41, 7, pp. 930–942, 1996.

[23] K. Kinosita, T. Sogo, and N. Adachi, "Iterative learning control using adjoint systems and stable inversion," *Asian J. Control*, vol. 4, pp. 60–67, 2002.

[24] D. Meng and K.L. Moore, "Robust iterative learning control for nonrepetitive uncertain systems," *IEEE Trans. Autom. Control*, vol. 62, no. 2, pp. 907–913, 2016.

[25] K.-S. Kim and Q. Zou, "A modeling-free inversion-based iterative feedforward control for precision output tracking of linear time-invariant systems," *IEEE-ASME Trans. Mechatron.*, vol. 18, no. 6, pp. 1767–1777, 2012.

[26] X. Yu, Z. Hou, M. M. Polycarpou, and L. Duan, "Data-driven iterative learning control for nonlinear discrete-time mimo systems," *IEEE Trans. Neural Netw. Learn. Syst.*, vol. 32, no. 3, pp. 1136–1148, 2020.

[27] Y. Chen, W. Jiang, and T. Charalambous, "Machine learning based iterative learning control for non-repetitive time-varying systems," *arXiv preprint arXiv:2107.00421*, 2021.

[28] W. Liu, L. Cheng, Z.-G. Hou, J. Yu, and M. Tan, "An inversion-free predictive controller for piezoelectric actuators based on a dynamic linearized neural network model," *IEEE-ASME Trans. Mechatron.*, vol. 21, no. 1, pp. 214–226, 2015.

[29] S.P. Diwan and S.S. Deshpande, "Computationally efficient nonlinear model predictive controller using parallel particle swarm optimization," *Bull. Pol. Acad. Sci. Tech. Sci.*, vol. 70, no. 4, p. e140696, 2022.

[30] A.T. Peebles, K.R. Ford, J.B. Taylor, J.M. Hart, L.P. Sands, and R.M. Queen, "Using force sensing insoles to predict kinetic knee symmetry during a stop jump," *J. Biomech.*, vol. 95, p. 109293, 2019.

[31] K.E. Renner, D.B. Williams, and R.M. Queen, "The reliability and validity of the loadsol® under various walking and running conditions," *Sensors*, vol. 19, no. 2, p. 265, 2019.

[32] W. Seiberl, E. Jensen, J. Merker, M. Leitel, and A. Schwirtz, "Accuracy and precision of loadsol® insole force-sensors for the quantification of ground reaction force-based biomechanical running parameters," *Eur. J. Sports Sci.*, vol. 18, no. 8, pp. 1100–1109, 2018.

[33] G.T. Burns, J. Deneweth Zendler, and R.F. Zernicke, "Validation of a wireless shoe insole for ground reaction force measurement," *J. Sports Sci.*, vol. 37, no. 10, pp. 1129–1138, 2019.

[34] J.C. Principe, N.R. Euliano, and W.C. Lefebvre, *Neural and adaptive systems: fundamentals through simulations with CD-ROM*. John Wiley & Sons, Inc., 1999.